MNRAS **452,** 2773–2787 (2015) doi:10.1093/mnras/stv1419

On the formation and evolution of the first Be star in a black hole binary MWC 656

M. Grudzinska,[1★] K. Belczynski,[1†] J. Casares,[2,3] S. E. de Mink,[4] J. Ziolkowski,[5] I. Negueruela,[6] M. Ribó,[7‡] I. Ribas,[8] J. M. Paredes,[7] A. Herrero[2,3] and M. Benacquista[9]

[1]*Astronomical Observatory, University of Warsaw, Al. Ujazdowskie 4, PL-00-478 Warsaw, Poland*
[2]*Instituto de Astrofisica de Canarias, E-38205 La Laguna, S/C de Tenerife, Spain*
[3]*Departamento de Astrofisica, Universidad de La Laguna, E-38206 La Laguna, S/C de Tenerife, Spain*
[4]*Anton Pannekoek Astronomical Institute, University of Amsterdam, NL-1098 HX Amsterdam, the Netherlands*
[5]*Nicolaus Copernicus Astronomical Center, Bartycka 18, PL-00-716 Warsaw, Poland*
[6]*Departamento de Fisica, Ingenieria de Sistemas y Teoria de la Senal, Universidad de Alicante, Apartado, 99, E-03080 Alicante, Spain*
[7]*Departament d'Astronomia i Meteorologia, Institut de Ciències del Cosmos, Universitat de Barcelona, IEEC-UB, Martí i Franquès 1, E-08028 Barcelona, Spain*
[8]*Institut de Ciencies de l'Espai – (IEEC–CSIC), Campus UAB, Facultat de Ciencies, Torre C5 – parell – 2a planta, E-08193 Bellaterra, Spain*
[9]*Center of Gravitational Wave Astronomy, University of Texas at Brownsville, Brownsville, TX 78520, USA*

Accepted 2015 June 22. Received 2015 June 10; in original form 2015 April 13

ABSTRACT

We find that the formation of MWC 656 (the first Be binary containing a black hole) involves a common envelope phase and a supernova explosion. This result supports the idea that a rapidly rotating Be star can emerge out of a common envelope phase, which is very intriguing because this evolutionary stage is thought to be too fast to lead to significant accretion and spin up of the B star. We predict ∼10–100 of B-BH binaries to currently reside in the Galactic disc, among which around 1/3 contain a Be star, but there is only a small chance to observe a system with parameters resembling MWC 656. If MWC 656 is representative of intrinsic Galactic Be-BH binary population, it may indicate that standard evolutionary theory needs to be revised. This would pose another evolutionary problem in understanding black hole (BH) binaries, with BH X-ray novae formation issue being the prime example. Future evolution of MWC 656 with an ∼5 $M_\odot$ BH and with an ∼13 $M_\odot$ main-sequence companion on an ∼60 d orbit may lead to the formation of a coalescing BH–NS (neutron star) system. The estimated Advanced LIGO/Virgo detection rate of such systems is up to ∼0.2 yr^{-1}. This empirical estimate is a lower limit as it is obtained with only one particular evolutionary scenario, the MWC 656 binary. This is only a third such estimate available (after Cyg X-1 and Cyg X-3), and it lends additional support to the existence of so far undetected BH–NS binaries.

Key words: stars: evolution – X-rays: binaries.

1 INTRODUCTION

We know at present 184 X-ray binaries (XRBs) consisting of a Be star and a compact object – Be XRBs (Ziolkowski 2014). Until the previous year, whenever the nature of the compact component was determined (in 119 systems), it was always a neutron star (NS). Not a single Be system containing a black hole (BH) was found during 40 years of observations of Be XRBs. Last year the first such system was finally found by Casares et al. (2014). This discovery motivated us to investigate the possible evolutionary scenarios leading to the formation of similar systems.

1.1 Be stars

Be stars are massive, not substantially evolved, main-sequence (MS) stars of spectral types B0–A0 with Balmer emission lines (Porter & Rivinius 2003). This range of spectral types corresponds roughly to a mass range of about 3–18 $M_\odot$. The emission lines (which give the name to this class of stars) originate in an outflowing viscous disc (excretion disc) around the star. Such a disc is very similar to the well-known viscous accretion discs, except for the changed sign of the rate of the mass flow. The excretion discs evolve dynamically

★E-mail: mgrudzinska@astrouw.edu.pl
†Warsaw Virgo Group.
‡Serra Húnter Fellow.

on a time-scale of a few years to few decades. In the course of this evolution, the disc undergoes a global one-armed oscillation instability (Kato 1983), manifesting itself in the form of the well-observed, so-called, *V*/*R* variability. This instability (progressing density waves) leads eventually to the disruption of the disc. A disc-less phase (with no emission lines) follows then, until the disc refills again (which takes years to decades; Porter & Rivinius 2003). The excretion discs were successfully modelled (Hummel & Vrancken 1995; Okazaki 1996; Hummel & Hanuschik 1997; Okazaki 1997; Porter 1999; Negueruela & Okazaki 2000, 2001) and these modellings helped to explain many observed properties of Be stars (both solitary ones and those that are members of binaries, in particular, XRBs).

1.2 Fraction of Be stars among B stars

At first, we would like to comment on the notion that the same star might show a Be phenomenon (and so be a Be star) over some intervals of time and not to show it (and so be a 'normal' B star) over some other intervals. It is quite likely, that a 'normal' B star in the course of its evolution is spun up and develops a Be phenomenon. However, it is clear that there are B stars (majority of them) that *are not* Be stars and that there are Be stars that show Be phenomenon during all time we observed them. They exhibit disc-less phases, which may last decades (Porter & Rivinius 2003). Such phases are part of a Be phenomenon and the stars do not stop being Be stars (at least, this is the accepted convention).

After this clarification, let us estimate how large a fraction of all B stars are Be stars. Abt (1987) found that Be stars comprise 18 per cent of the B0–B7 stars in a volume-limited sample of field stars (with a maximum Be fraction for the spectral types B3–B4). A similar result was obtained by Zorec & Briot (1997) who found the fraction of Be stars to be 17 per cent for the Galactic field stars (this was a mean value; a maximum of 34 per cent was found for the spectral type B1). The percentage of Be stars was estimated also for stellar clusters. Keller, Wood & Bessell (1999) investigated the frequency of Be stars in six young clusters in the Magellanic Clouds. They found a range of 13–34 per cent. Maeder, Grebel & Mermilliod (1999) investigated 21 clusters in the interior of the Galaxy, the exterior of the Galaxy, the LMC and the SMC and found the fractions of, respectively, 11, 19, 23 and 39 per cent. The similar investigation carried out by Wisniewski & Bjorkman (2006) brought similar results (the ranges of Be fractions were 9–39 per cent for earlier type (B0–B3) Be stars and 3–32 per cent for later (B4–B5) types). McSwain & Gies (2005) analysed 48 open clusters and found the mean (for all clusters) percentage of Be stars equal to 7.1 per cent (with a maximum of ∼11 per cent for spectral types B2–B3). They compare it with Abt's value and attribute the difference to the selection effects in Abt's estimate (a bias towards earlier B spectral types). Fabregat & Torrejón (2000) analysed seven 'Be rich' clusters in Milky Way and in the Magellanic Clouds. They found very high percentage: 21 to ∼50 per cent. Another 'Be-rich' cluster was investigated by Marco & Negueruela (2013) who found very high (∼40 per cent) fraction of Be stars close to the turn-off (spectral type B1) but very few Be stars for later spectral types.

To summarize, the fraction of Be stars among B stars is about 20–30 per cent, generally increasing for earlier spectral types. If we consider Be XRBs, one should remember that Be stars in XRBs have somewhat earlier spectral types than solitary Be stars (see the further text), which may indicate that the factor $f_{\rm Be}$ (the fraction of XRB containing a Be star) should be somewhat higher – perhaps 30 per cent.

1.3 The origin of fast rotation of Be stars

There is little doubt that all distinct properties of Be stars are related to the presence of an outflowing excretion disc. There is also little doubt that the presence of these discs is related to the fast rotation of these stars. Struve (1931) suggested that this rotation is very close to the critical (or break-up) equatorial velocity. Later, a canonical view was established (Porter 1996; Chauville et al. 2001) according to which the rotation is significantly subcritical with equatorial velocity equal only 70–80 per cent of the critical velocity. However, more recently Townsend, Owocki & Howarth (2004) and Ekström et al. (2008) gave arguments indicating that the rotation might be indeed very close to critical, with equatorial velocity smaller only by a few per cent (and not 20–30 per cent) than the critical one. Such fast velocity makes the formation and maintaining of the excretion disc much more likely (Granada et al. 2013).

As for the origin of fast rotation, Martayan et al. (2006) indicated that Be stars are born with higher initial (on ZAMS) rotation than other B stars. It seems, however, that they are not born as Be stars from the very beginning. Rather, the higher initial rotation facilitates the action of mechanisms that later spin up these stars to nearly critical rotation. Two such major mechanisms were considered.

One of them is the evolutionary spin up during the MS evolution. The reason for the spin-up is the significant decreasing of the moment of inertia of the star during this phase of evolution. This explanation might be supported by the fact the Be phenomenon seems to be associated with the second half of the MS evolution of B stars (McSwain & Gies 2005; Frémat et al. 2006). The first mechanism was discussed and modelled by different authors (Meynet & Maeder 2005; Ekström et al. 2008; Granada et al. 2013). The general conclusion of these modellings is that evolutionary spin up is sufficient to explain the Be phenomenon.

The second mechanism is the spin up due to accretion in a binary system. Initially, this scenario was proposed for the formation of Be-XRBs (e.g. Rappaport & van den Heuvel 1982). This scenario can also account for single Be stars, due to disrupted binary systems or binary mergers. First estimates of the importance of this scenario were provided by Waters et al. (1989), Pols et al. (1991) and Portegies Zwart (1995). More recent simulations accounting for the actual spin-up process and mergers were performed by de Mink et al. (2013). The general view of the advocates of the binary mechanism is that this scenario can account for the majority of the Be stars. For example, McSwain & Gies (2005) concluded that more than 70 per cent of all Be stars had to be spun up in the process of accretion in binary systems. de Mink et al. (2013) and Shao & Li (2014) both conclude that all Be stars can be accounted for by the binary evolution. Especially, if mergers of short-period contact binaries are taken into account.

The summary of this controversy is difficult. It seems possible that both mechanisms are at work and that, at present, it is not possible to estimate reliably the relative importance of each formation channel.

1.4 Be stars in XRBs

Be stars in XRBs are, in many respects, similar to isolated Be stars. They have excretion discs which develop one-armed oscillations and display *V*/*R* variability. The dynamical evolution of their discs includes the disruption of the disc and the following disc-less phase.

However, there are also notable differences. The first concerns the spectral types. Be stars in XRBs have, on average, earlier spectral types than isolated Be stars (Negueruela 1998). The range is O9–B3 as opposed to B0–A0 for isolated Be stars. It indicates that

also masses of Be stars in XRBs are somewhat higher (perhaps 6–24 $M_\odot$ instead of 3–18 $M_\odot$). The second major difference concerns the excretion discs. The discs in XRBs interact with the compact companions (almost always NSs). This interaction leads to the appearance and the growth in the certain locations in the disc of the resonances between Keplerian frequencies of the disc matter and the orbital frequency of the NS. These resonances lead to the tidal truncation of the disc (Artymowicz & Lubow 1994; Negueruela & Okazaki 2000, 2001; Okazaki & Negueruela 2001). Tidal truncation makes the discs in Be XRBs smaller and denser than the discs around isolated Be stars (Reig, Fabregat & Coe 1997; Negueruela & Okazaki 2001).

1.5 Be X-ray binaries

Be X-ray binaries (Be XRBs) are the most numerous class among high-mass X-ray binaries. We know at present 184 Be XRBs and only about 60 other high-mass XRBs (both Galactic and extragalactic systems are included in this statistics; Ziolkowski 2014). In 119 of Be XRB systems, the X-ray pulsations are observed, confirming that the compact component must be an NS. The pulse periods are in the range of 34 ms to ∼ 1400 s (Ziółkowski & Belczyński 2011). Until the previous year not a single Be system containing a BH was found. The Be XRBs are rather wide systems (orbital periods in the range of ∼10–1180 d; Ziolkowski 2014). The orbits are frequently eccentric. A compact component accretes from the excretion disc of a Be star (earlier known as the equatorial wind of a Be star).

The X-ray emission from Be XRBs (with a few exceptions) is of a distinctly transient nature with rather short (days to weeks) active phases separated by much longer (months to tens of years) quiescent intervals (a typical flaring behaviour). There are two types of flares, which are classified as Type I outbursts (smaller and roughly regularly repeating) and Type II outbursts (larger and irregular). This classification was first defined by Stella, White & Rosner (1986). Type I bursts are observed in systems with highly eccentric orbits. They occur close to periastron passages of an NS. They are repeating at intervals $\sim P_{\rm orb}$. Type II bursts may occur at any orbital phase. They are correlated with the disruption of the excretion disc around Be star. They repeat on time-scale of the dynamical evolution of the excretion disc (∼ few years to few tens of years). This recurrence time-scale is generally much longer than the orbital period (Negueruela et al. 2001).

Be XRBs systems are known to contain two discs: an excretion disc around the Be star and an accretion disc around the NS. Both discs are temporary: the excretion disc disperses and refills on time-scales ∼ few years to few decades (dynamical evolution of the disc; Porter & Rivinius 2003), while the accretion disc disperses and refills on time-scales ∼ weeks to years (which is related either to the orbital motion of an NS on an eccentric orbit or to the disruption episodes of the excretion disc). Formation of the accretion discs was analysed by Hayasaki & Okazaki (2006) and Cheng et al. (2014).

The more detailed description of the properties of Be XRBs is given, e.g. in Negueruela et al. (2001), Ziolkowski (2002), Belczynski & Ziolkowski (2009), Ziółkowski & Belczyński (2011), Reig (2011) and references therein.

The fact that we observe over one hundred NS Be XRBs and not a single BH Be XRB, became known as the problem of the missing BH Be XRBs. Trying to explain the reasons for which we do not observe BH Be XRBs, Belczynski & Ziolkowski (2009) carried out stellar population synthesis calculations aimed at estimating the ratio of NS to BH Be XRBs, expected on the basis of the stellar evolution theory. The results of their calculations predict that for our Galaxy the expected ratio of Be XRBs with NSs to the ones with BHs $F_{\rm NS/BH}$ should be, most likely, equal ∼54. Since we know 48 NS Be systems in the Galaxy, then it comes out that the expected number of BH systems should be just one. It seems that this system was just found (Casares et al. 2014).

2 MODELING

2.1 The STARTRACK code

We use the STARTRACK population synthesis code (Belczynski, Kalogera & Bulik 2002; Belczynski et al. 2008) to generate a population of binaries in the Galaxy. The code is based on revised formulas from Hurley, Pols & Tout (2000), among other with updated wind mass loss prescriptions, and calibrated tidal interactions, physical estimation of donor's binding energy (λ) and convection-driven, neutrino-enhanced supernova (SN) engines. A full description of the code can be found in the papers mentioned above. Here we concentrate only on these aspects that are important from the viewpoint of modelling used in this study.

The initial parameters of systems simulated with the STARTRACK are randomly chosen from the following distributions:

(i) three component broken power-law initial mass function with slope of −1.3 for initial mass $M_{\rm zams}$ = 0.08–0.5 $M_\odot$, −2.2 for $M_{\rm zams}$ = 0.5–1 $M_\odot$, −2.7 for $M_{\rm zams}$ = 1–150 $M_\odot$ (Kroupa & Weidner 2003);
(ii) flat mass ratio distribution in range q = 0–1 (Kobulnicky, Fryer & Kiminki 2006);
(iii) flat in the logarithmic distribution of initial binary separations (Abt 1983) $\propto 1/a$ in range from a minimum value, to prevent stars from filling their Roche lobes at zero age, up to 10^5 $R_\odot$;
(iv) thermal-equilibrium distribution of eccentricities (Duquennoy & Mayor 1991) $\Xi(e) = 2e$ in the range 0–1.

The binary fraction is assumed to be 50 per cent (i.e. 2/3 of stars are in binaries). We note that recently measured initial distributions for O stars (Sana et al. 2012) are different from those employed in our study. However, it was demonstrated that a change of distributions from the ones used here to the new ones does not significantly affect predictions for progenitors of double compact objects (de Mink & Belczynski, in preparation).

Among the most important physical mechanisms driving binary evolution is the common envelope (CE) phase. The CE is very efficient in creating close binaries. The outcome of this evolutionary phase can be described by the energy balance formula (Webbink 1984):

$$\alpha_{\rm CE}\left(\frac{GM_{\rm don,f}M_{\rm acc}}{2A_{\rm f}}-\frac{GM_{\rm don,i}M_{\rm acc}}{2A_{\rm i}}\right)=\frac{GM_{\rm don,i}M_{\rm don,env}}{\lambda R_{\rm don,lob}}, \qquad (1)$$

where $M_{\rm don}$ and $M_{\rm acc}$ are masses of donor and accretor, respectively; $M_{\rm don,\,env}$ is mass of the envelope of the accretor; A is a binary separation; $R_{\rm don,\,lob}$ is a Roche lobe radius of the donor at the beginning of mass transfer. Index *i/f* indicates the initial/final (before/after CE) value of a given quantity. The λ parameter describes the binding energy of the envelope of the donor and in the current version of code we use the 'Nanjing' λ (Xu & Li 2010a,b) with specific implementation into the STARTRACK code described in Dominik et al. (2012). The $\alpha_{\rm CE}$ parameter describes the efficiency of the transfer of orbital energy into the envelope. We allow for large variation of this parameter.

Another important phase in the past evolution of binaries is the core-collapse/SN explosion. Due to its potential asymmetry, the new born compact object (NS or BH) may receive a natal kick. According to the observed velocities of radio pulsar (Hobbs et al. 2005), we choose the maximum kick velocity from the single Maxwellian distribution with $\sigma = 265$ km s^{-1}. This value can be reduced depending on the fallback factor ($f_{\rm fb}$), which describes percentage amount of matter ejected during SN and accreted back on to the compact object:

$$V_k = V_{\rm max}(1 - f_{\rm fb}). \quad (2)$$

This prescription is used for NSs and BH, but most of the former receive full natal kicks, with exception of electron capture SN (ECSN) for which we adopt no natal kicks at all. The full description of double compact object formation and rationale behind it is given by Fryer et al. (2012) and Belczynski et al. (2012b).

2.2 The standard model

In the standard model, we employ energy balance for CE evolution with fully efficient transfer of orbital energy to the envelope energy ($\alpha = 1$). The maximum natal kicks velocities are drawn from the Maxwellian distribution with $\sigma = 256$ km s^{-1}. Fallback factor $f_{\rm fb}$ varies in range 0–1 (from full kick for 0 to no kick for 1). The SN explosion mechanism for the standard model is a convection-driven, neutrino-enhanced engine (Fryer et al. 2012). The explosion occurs within the first 0.1–0.2 s (so-called 'rapid' explosion). This engine reproduces (Belczynski et al. 2012b) the observed Galactic XRB mass gap (Bailyn et al. 1998; Özel et al. 2010). All results that we present are obtained for the metallicity typical of the solar neighbourhood $Z = 0.02$ and presented for a specific assumption on CE outcome: all donors beyond MS are allowed to survive CE (but see Belczynski et al. 2007, 2010c for an alternative scenario for Hertzsprung Gap donors). Full description of the standard evolutionary model can be found in Dominik et al. (2012).

We only evolved binaries with primaries in mass range 6–150 $M_\odot$ and secondaries in mass range 1–150 $M_\odot$, as lower mass binaries may have only a very little chance to produce binaries containing a BH. We only follow stars in the Galactic disc for which we assume a constant star formation at the level of 3.5 $M_\odot$ yr^{-1} over 10 Gyr.[1] We have evolved 10^8 binaries which gives us one full realization of the Galactic disc. We then use *Monte Carlo* techniques to evaluate the probability of catching each system during B-BH phase at the current time in the Galactic disc. A fraction $f_{\rm Be}$ of B-BH binaries belong to the interesting group of Be-BH systems (see Section 1.2).

2.3 Variations on the standard model

We also check the sensitivity of our predictions to parameters that are important for the formation and evolution of B-BH binaries.

In models V_1 and V_2, we change the $\alpha_{\rm CE}$ value to 0.1 and 5, respectively. In model V_3 all BH do not receive any natal kicks during SN explosion. In model V_4 we change the mechanism of SN explosion from the 'rapid' explosion to the 'delayed' one. In delayed SN engine, the explosion can occur as late as 1 s after bounce. This scenario, unlike the 'rapid' one, produces a continuous mass spectrum of compact objects, and the observed mass gap must then be a result of some observational bias (e.g. Kreidberg et al. 2012).

2.4 Definition of B-BH and MWC 656-like systems

Due to large uncertainties in rotation physics, we choose not to use rotation as a qualifier for the Be phenomenon. Initial rotation of massive stars is not yet fully constrained, angular momentum gain during accretion in massive binaries is not fully understood and angular momentum loss with stellar winds for massive stars is still uncertain (see Section 4 for a more detailed discussion). Therefore, we study a broad spectrum of massive stars with BH, to which we refer as B-BH binaries and which are defined below. Some of these binaries may produce or are born with Be or Oe star.

In our simulation B-BH systems are binaries satisfying a following criterion:

$$\begin{aligned} &\text{BH} + \text{MS binary} \\ &10 < P_{\rm orb} < 1200\,\text{d} \\ &3 < \text{MS mass} < 30\,M_\odot. \end{aligned} \quad (3)$$

Note that this specific choice of orbital periods along with MS secondaries leads to population of wind-fed binaries. We have chosen the orbital periods such that they are within the expected range for Be XRBs (see Section 1.5). Also note that MS mass range includes not only B stars (<15 $M_\odot$) but also some O stars as to correspond to the observed Be/Oe population (Negueruela 1998 and references therein).

We also define a subpopulation of B-BH binaries with properties similar to these observed for MWC 656 Casares et al. (2014) as

$$\begin{aligned} &\text{BH} + \text{MS binary} \\ &55 < P_{\rm orb} < 65\,\text{d} \\ &3.8 < M_{\rm BH} < 6.9\,M_\odot \\ &10 < M_{\rm MS} < 16\,M_\odot \\ &e < 0.5. \end{aligned} \quad (4)$$

The masses have been chosen within the 1σ limits determined by Casares et al. (2014); the eccentricity range was established in a private communication with the team which discovered the first BH+Be binary; the range for the orbital period was chosen arbitrarily.

Note that to obtain the information on Be-BH systems or systems similar to MWC 656 containing a Be star, all numbers/rates we get for the groups defined above need to be multiplied by a factor $f_{\rm Be}$, which is not well known. If the fraction of systems where the B star shows the Be phenomenon were similar to the observed fraction in Milky Way and Magellanic Clouds clusters, the reduction factor $f_{\rm Be}$ would be about 0.3 (see Section 1.2).

3 RESULTS

In the following text we refer to initially more massive star as primary (BH progenitor), and initially less massive star (MS star that is potential Be or Oe object) as secondary.

[1] Diehl et al. (2006), Misiriotis et al. (2006) and Robitaille & Whitney (2010) find a total star formation rate (SFR) to be 4, 2.7 and ~1 $M_\odot$ yr^{-1}, respectively. A study by Kennicutt (1998) suggests SFR value in the range 0–10 $M_\odot$ yr^{-1}. Additionally, if we assume a constant SFR over the period of 10 Gyr then the Galactic disc mass provided by McMillan (2011) divided by this period gives an average SFR ≈6.5 $M_\odot$ yr^{-1}. Thus, the value of SFR chosen for our study (3.5 $M_\odot$ yr^{-1}) is within reasonable limits.

3.1 Overall properties of B-BH binaries

The total number of B-BH systems formed in our standard model simulations over entire 10 Gyr of evolution of the Galactic disc is $N^{\rm form}_{\rm B\text{-}BH} = 8700$, while number of MWC 656-like systems is $N^{\rm form}_{\rm MWC656} = 13$.

Note that our predictions for MWC 656-like systems are subject to errors from small number statistics. But these errors are smaller than ones associated with evolutionary uncertainties. Various systems that we generate have a range of lifetimes during B-BH (with an average of ∼45 Myr) or MWC 656 (with an average of ∼6 Myr) stage. We use the lifetime of each system to assess the probability that it is present in the current Galactic disc population. We use $N = 10^4$ of Monte Carlo realizations of the formation time (drawn from uniform distribution) of a given system in range 0–10 Gyr and check how many times n a given system is present at the current Galactic age (10 Gyr). The current number of given binary population is given by n/N. This number may be smaller than one and then it indicates how low is the probability of one system to exist in the current predicted population.

The total number of B-BH systems found in our simulations to be present at the current moment in the Galactic disc is $N^{\rm curr}_{\rm B\text{-}BH} = 39$, while number of MWC 656-like systems is well below one: $N^{\rm curr}_{\rm MWC656} = 0.007$ (i.e. the probability of having one system at present is ∼1 per cent).

In Figs 1, 2, 3 and 4, we show distributions of orbital period, BH mass, companion mass and orbital eccentricity for B-BH binaries (defined by equation 3). We also show a subpopulation of B-BH binaries that resemble the observed properties of MWC 656 (defined by equation 4). In Figs 5 and 6, we show the two-dimensional distributions of orbital period versus B star mass and eccentricity versus BH mass for B-BH binaries. With a white rectangle we mark the region corresponding to systems defined as MWC 656-like (equation 4). In Fig. 7, we present the sensitivity of total number of MWC 656-like systems formed over entire 10 Gyr in the Galaxy on the adopted orbital period range in the systems' definition equation (4).

There is a two-stage evolution leading to the formation of B-BH binaries; CE followed by core-collapse/SN (forms BH). In the first stage the massive primary expands after MS and initiates Roche Lobe overflow (RLOF). Due to the high mass ratio (typically $M_{\rm primary}/M_{\rm secondary} \gtrsim 3$) mass transfer is unstable and leads to CE.

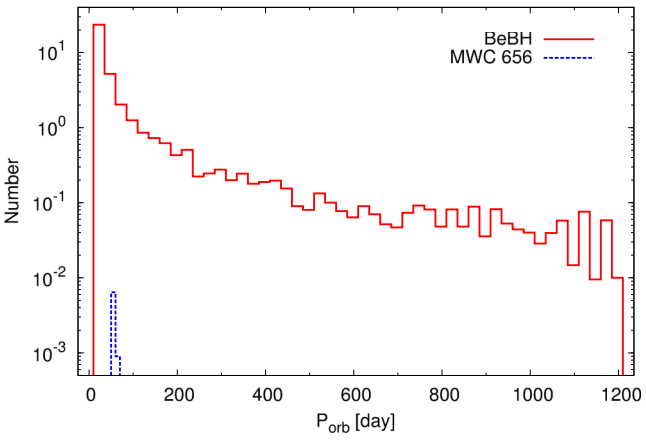

Figure 1. Orbital period distribution for overall group of B-BH binaries (red solid line) and MWC 656-like subpopulation (blue dashed line). Predicted current Galactic populations are shown. Note that overall number of B-BH binaries (39) is much larger than for MWC 656-like systems (0.01 – it is a probability of having one MWC 656-like system).

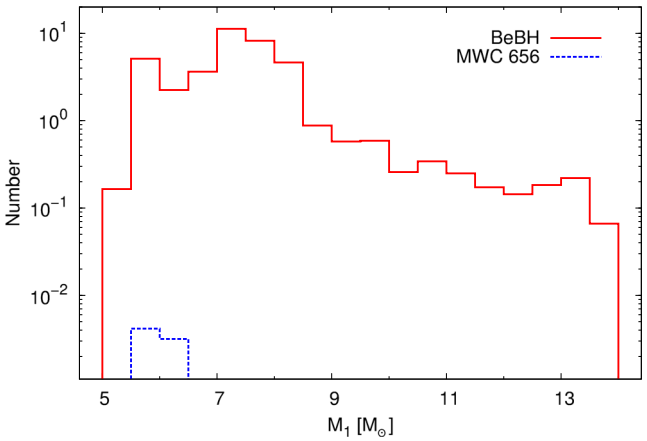

Figure 2. BH mass distribution for overall group of B-BH binaries (red solid line) and MWC 656-like subpopulation (blue dashed line). Predicted current Galactic populations are shown.

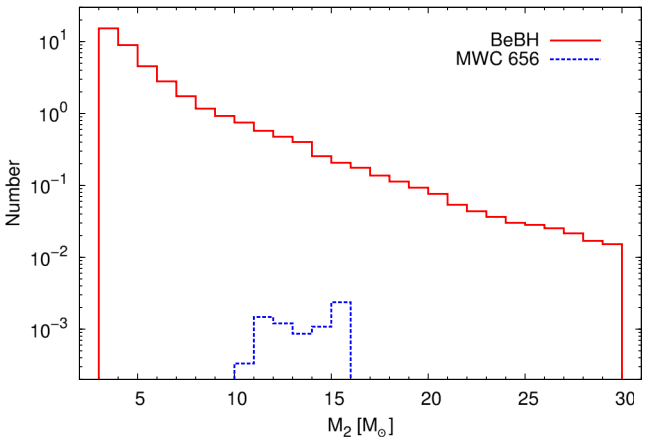

Figure 3. B star mass distribution for overall group of B-BH binaries (red solid line) and MWC 656-like subpopulation (blue dashed line). Predicted current Galactic populations are shown.

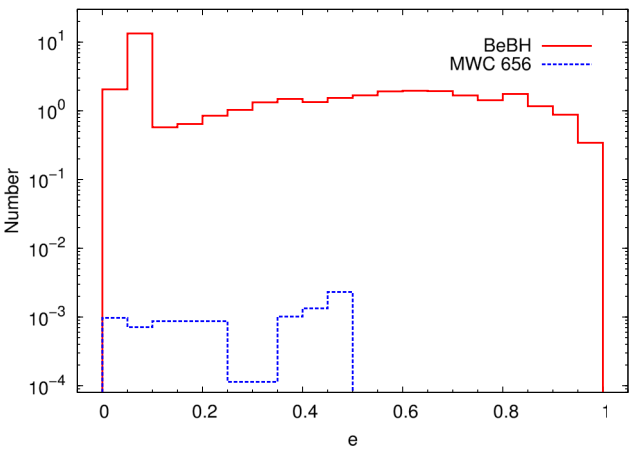

Figure 4. Eccentricity distribution for overall group of B-BH binaries (red solid line) and MWC 656-like subpopulation (blue dashed line). Predicted current Galactic populations are shown.

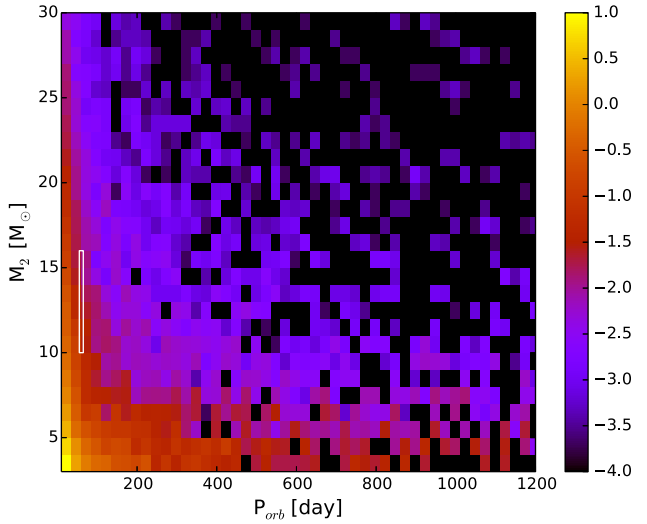

Figure 5. Two-dimensional distribution of orbital period (*x*-axis) and B star mass (*y*-axis) for B-BH binaries. The numbers next to the colour bar indicate the logarithm of the predicted current Galactic B-BH population. The white rectangular box indicates the area of MWC 656-like systems defined in equation (4).

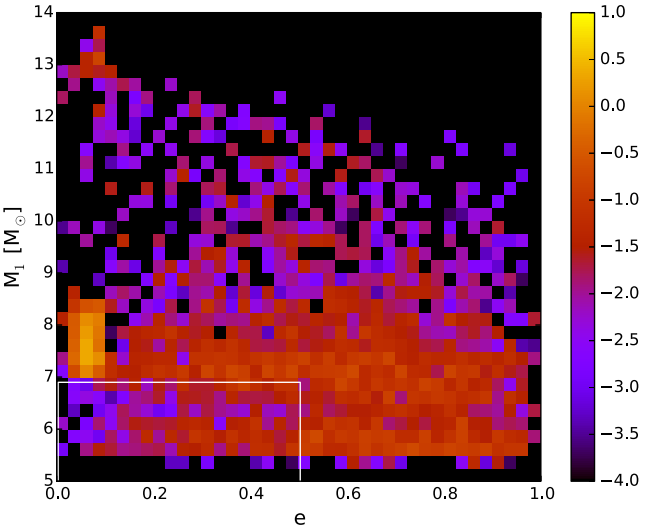

Figure 6. Two-dimensional distribution of eccentricity (*x*-axis) and BH mass (*y*-axis) for B-BH binaries. The numbers next to the colour bar indicate the logarithm of the predicted current Galactic B-BH population. The white rectangular box indicates the area of MWC 656-like systems defined in equation (4).

At the onset of CE, our massive primary (∼30–60 $M_\odot$) is most likely (∼90 per cent) in the core helium burning (CHeB) phase and has a well-developed convective envelope. Only in a relatively small number of cases (∼10 per cent) the primary is on the Hertzsprung gap (HG) with either a radiative or shallow convective envelope.[2]

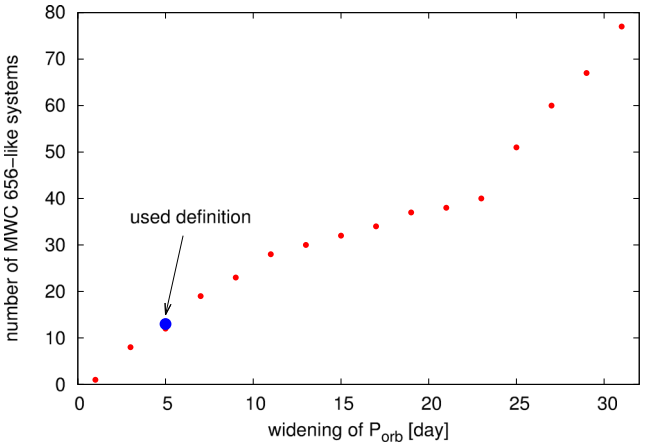

Figure 7. Sensitivity of formation efficiency of MWC 656-like systems (as defined in equation 4). For our study we have adopted definition $55 < P_{\rm orb} < 65$ d for MWC 656-like systems in respect to orbital period. For this definition, we produce 13 systems in entire 10 Gyr of Galaxy evolution (see the blue dot). If we widen the period range by a given number of days (horizontal coordinate) on both sides of the measured orbital period of MWC 656 ($P_{\rm orb} = 60.37$ d), then we obtain specific number of MWC 656-like systems (vertical coordinate).

In the case of HG donor, it is not at all clear whether CE develops at all even for high mass ratios (unpublished MESA simulations). This 90–10 per cent division is an evolutionary selection effect. The secondary star is typically of much lower mass (∼5–15 $M_\odot$; see Fig. 3) than primary. Therefore, it is easier for a binary to survive the CE phase for small CE envelope mass. HG stars have massive and tightly bound envelopes, while the envelope mass and binding energy decreases rapidly during CHeB phase. Both as a result of expansion and for high metallicity also due to intense wind mass loss. After CE initially wide systems evolve to much shorter orbital periods (∼10–100 d; see Fig. 1). Massive primaries lose their entire H-rich envelope, and become Wolf–Rayet stars. We assume that CE is very rapid and that the MS secondary does not have time to accrete. In our simulations we allow only compact objects (NS and BH) to accrete a small but significant amount of mass during CE. Note that at the moment the CE phase is far from being understood (see however Ivanova et al. 2013) and our *assumptions* on accretion physics in CE are subject to verification.

In the second stage, the Wolf–Rayet star explodes in Type Ib/c SN and forms a BH. Alternatively, for very massive stars we assume direct BH formation without accompanying SN. Our models for single stars allow for Wolf–Rayet star formation above $M_{\rm zams} \sim 20\,M_\odot$ and for direct BH above $M_{\rm zams} \sim 40\,M_\odot$. RLOF episodes in binaries may significantly shift these boundaries up or down depending on a given binary configuration and evolutionary stage of its components. The associated-with SN neutrino losses and potential mass loss and natal kick affect the orbit (altering eccentricity and the semimajor axis). A BH binary with MS companion is formed. Such

[2] Note that these numbers have changed significantly since Belczynski & Ziolkowski (2009), who reported only ∼4 per cent of progenitors of B-BH binaries to go through CE with a donor on CHeB stage. This apparent discrepancy is a direct consequence of updates of input physics made in STARTRACK code. It mostly originates from change of CE physics. In the updated code, the iλ parameter that describes the binding energy of the donor star is calculated based on stellar radius, metallicity and evolutionary stage. In the previous study, the authors used a constant value $\lambda = 1$, which is now replaced with a typical physical value of ∼0.1–0.2 for BH progenitors on HG (see fig. 3 in Dominik et al. 2012). It means, that now λ is too small to allow HG donor to survive CE, and these systems now are found to typically merge during CE. The smaller lambda values preferentially select donors with small envelope mass to survive CE. For massive BH progenitors stars lose their H-rich envelopes during CHeB and that is what we note in our new results.

a binary may either fall right within our criteria for B-BH or MWC 656-like object directly, or it may evolve to satisfy these criteria at a later stage. The only process altering the binary orbit at this stage is wind mass loss from the MS star increasing the orbital separation (but this effect is very small for the MS stars in the mass range we consider). For close binaries tidal interactions (synchronizing MS stars and circularizing the orbit) also play a role. Since we have chosen our lower limit on the orbital period to be rather large (10 d), the systems that are subject to efficient tidal interactions are not typical progenitors of B-BH/MWC 656-like objects.

3.2 The formation of MWC 656-like system

Here, we present a typical evolutionary scenario that leads to the formation of a MWC 656-like system (see Fig. 8).

We start the binary evolution with two components on the zero-age main sequence (ZAMS) with $M_1 = 41\,\mathrm{M}_\odot$ (primary) and $M_2 = 14\,\mathrm{M}_\odot$ (secondary). The initial semimajor axis of the orbit is $a = 5.3 \times 10^3\,\mathrm{R}_\odot$ and its eccentricity is $e = 0.42$ (the orbital period is $P_{\rm orb} = 6000$ d). After 4.8 Myr the primary with a mass $M_1 = 35\,\mathrm{M}_\odot$ finishes core hydrogen-burning and enters the HG. At this phase the primary significantly expands and tidal forces begin to circularize the orbit. Next, the primary enters CHeB expanding towards its Roche lobe. The orbit becomes fully circularized. This phase ends with the primary ($M_1 = 17\,\mathrm{M}_\odot$) overfilling its Roche lobe and initiating the CE phase. At $t = 5.1$ Myr a close binary emerges out of the CE – an $M_1 = 13\,\mathrm{M}_\odot$ helium core of the primary on a relatively close orbit (separation decreases from $a = 5300$ to $142\,\mathrm{R}_\odot$ corresponding to decrease in orbital period from $P_{\rm orb} = 8000$ to 38 d) around the mostly unaffected MS secondary $M_2 = 14\,\mathrm{M}_\odot$. After ∼0.35 Myr the helium star primary finishes nuclear burning and its mass decreases to $M_1 = 10\,\mathrm{M}_\odot$ due to strong Wolf–Rayet type winds. Just before the SN explosion the semimajor axis of the orbit is $a = 167\,\mathrm{R}_\odot$ and the orbital period $P_{\rm orb} = 52$ d (expansion due to the wind mass loss). The primary explodes in a Type Ib/c SN (ejected mass ∼2.5 $\mathrm{M}_\odot$) and forms a light BH with mass $M_1 = 5.6\,\mathrm{M}_\odot$ (we have assumed ∼10 per cent mass loss in neutrino emission). We obtain a natal kick from an asymmetric mass ejection scenario and for this particular system the magnitude of the kick is 130 km s^{-1} in such direction that it changes the separation to $a = 165\,\mathrm{R}_\odot$ ($P_{\rm orb} = 56$ d) and eccentricity to $e = 0.01$. Depending on the orientation of the kick, the post-SN eccentricity may vary in a broad range. For small post-SN eccentricities ($e < 0.1$) systems have a likely chance to form BH–NS binary at the end of evolution, while more eccentric systems tend to finish evolution in CE mergers (see Section 3.5). Over the next ∼9 Myr this relatively close binary remains almost unchanged with slight orbital expansion due to wind mass loss from the MS secondary ($a = 168\,\mathrm{R}_\odot$, $P_{\rm orb} = 58$ d). Throughout this phase the system is a wind-fed XRB and it meets our criteria equation (4) and we tag it as the MWC 656-like system.

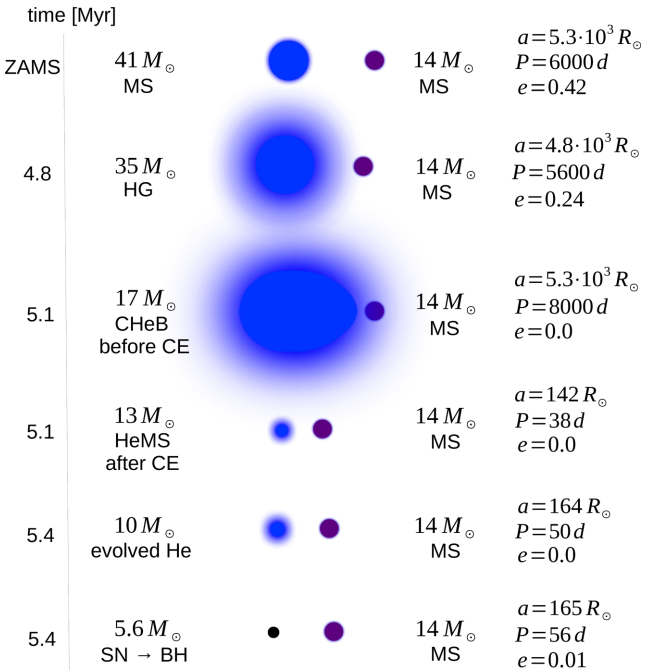

Figure 8. Typical evolution that may lead to the formation of MWC 656-like system. For the detailed description of the evolutionary history, see Section 3.2. Note that the two most important evolutionary factors are CE phase that brings orbital period close to the current observed value and SN Ib/c that forms rather light BH similar to the one residing in MWC 656. The notation: ZAMS – zero-age main sequence, MS – main sequence, HG – Hertzsprung gap, CHeB – core helium burning, HeMS – helium main sequence, BH – black hole, CE – common envelope, SN – super nova.

Initially, MWC 656 progenitors are two massive stars. If placed on a short orbit, such stars would begin interacting while on the MS or at the beginning of the HG and such an RLOF would most likely lead either to component merger (Sana et al. 2012) or would deplete the primary mass below the threshold of BH formation. For wide binaries, it takes a CE phase to decrease the orbital size to the currently observed period of MWC 656 (as described in our example). For very wide systems either CE is never encountered or if it is there is only very little mass in CHeB donor envelope and orbital decrease is not efficient enough to produce orbital period observed for MWC 656.

3.3 Parameter study

Our results are subject to a number of evolutionary uncertainties. We have performed several additional calculations that probe the most obvious uncertainties in the formation of B-BH binaries. In models V_1 and V_2, we have altered the energy balance in CE evolution that is required in all channels leading to B-BH binary formation. In models V_3 and V_4, we have changed our treatment of BH formation (natal kicks and BH mass). These changes lead to different formation efficiency of B-BH binaries. In Table 1, we list total number of B-BH binaries formed over entire 10 Gyr of Galactic evolution as well as their current predicted number in Galaxy for all models. The same numbers are listed for MWC 656-like systems.

The current number of B-BH systems is predicted at the level of ∼10–100. This number is rather sensitive to the adopted assumption on CE efficiency. For model in which we allow only 10 per cent

Table 1. B star + BH binary numbers in Milky Way.[a]

Model	MWC 656-like		B-BH		Comment
S_0	13	(0.007)	8, 700	(39)	Standard evolution
V_1	0	(0)	1, 600	(7)	$\alpha_{\rm CE} = 0.1$
V_2	34	(0.026)	55, 800	(131)	$\alpha_{\rm CE} = 5$
V_3	71	(0.063)	12, 800	(63)	No BH kicks
V_4	8	(0.004)	13, 300	(50)	Delayed SN engine

[a]The total number of B-BH and MWC 656-like systems formed in simulations over 10 Gyr of evolution of the Galaxy; in parenthesis we list the current number of systems in the Galaxy.

($\alpha_{\rm CE} = 0.1$; model V_1) of orbital energy to be used in CE ejection we predict only seven B-BH systems to be currently present in our Galaxy. For much more efficient ejection, with five times of orbital energy is used ($\alpha_{\rm CE} = 5.0$; model V_2) for CE ejection we find many more B-BH systems: 131. We only allow orbital energy to increase in such arbitrary way as to mimic the possibility that bounding energy of CE is much lower than used in current predictions. We use binding energy estimates from Xu & Li (2010a,b) that give binding energy of envelope for a given star radius, metallicity and star evolutionary stage. However, the envelope internal energy may lead to much easier ejection and it was estimated that it is potentially realistic to decrease binding energy by factor of ∼5 (Ivanova & Chaichenets 2011). That is what we have employed in model V_2. For our reference model we have used 100 per cent of orbital energy for CE ejection ($\alpha_{\rm CE} = 1.0$; model S_0).

Typical B-BH formation starts with a rather massive star (BH progenitor) that forms massive envelope after MS. Ejection of massive CE (10–30 $M_\odot$; at the end of HG) by a typical B star (∼5–15 $M_\odot$; see Fig. 3) is rather hard. In particular, for low ejection efficiency ($\alpha_{\rm CE} = 0.1$) it leads to a decrease in number B-BH binaries. For model in which we allow for lowered binding energy (or high $\alpha_{\rm CE} = 5.0$) the B-BH number increases. Alternatively, binary channels are naturally selected in which the envelope of a massive primary is depleted by evolution (winds and core growth) and then late case C RLOF leads to CE development (with CHeB donor) and B-BH formation.

The delayed SN model allows for the formation of low-mass BHs (see Fryer et al. 2012), as opposed to our standard model in which we do not allow formation of BHs in the mass gap: 3–5 $M_\odot$ (Belczynski et al. 2012b). We note no significant change in number of B-BH binaries between these two models (standard versus delayed SN). There is a small increase of B-BH binaries in the model with no BH kicks, since in this case some progenitors are not disrupted upon BH formation. Since the majority of BHs in B-BH binaries are predicted to have rather high mass (peak of mass distribution at 7–8 $M_\odot$; see Fig. 2) then they receive small or no natal kicks in our standard model. Therefore, the change to zero BH kick has a small effect on the overall B-BH population. This is quite different for MWC 656-like systems, for which we note factor of ∼10 increase of current Galactic number in model V_3. As low-mass BHs (as observed in MWC 656) receive non-zero kicks (binary disruptions) at the formation in our standard model, thus in model V_3 (no kicks) we note significant increase of MWC 656-like systems in the overall population of B-BH binaries.

We note that MWC 656 eccentricity and peculiar space velocity are consistent with no or small natal kick. The high BH natal kicks (above 100–150 km s^{-1}) may be excluded by the analysis presented in the appendix. In our particular example of the formation of MWC 656-like systems (presented in Fig. 8), the BH is formed with a moderate 3D natal kick $V_{\rm kick} = 130$ km s^{-1} and mass loss of ∼3 $M_\odot$. This natal kick was oriented in such a way that eccentricity was essentially not affected ($e_{\rm postSN} = 0.01$), but the systemic velocity was increased by 50 km s^{-1}. This is close to the values presented in the appendix: $e < 0.14$ and $V_{\rm spaceMWC656} < 37.4$ km s^{-1}. Within our population of MWC 656-like systems we find binaries that are fully consistent (in a 1σ range) with the appendix estimates: (i) for natal kick of 23 km s^{-1} and mass loss of ∼3 $M_\odot$ we get $e = 0.1$ and $V_{\rm spaceMWC656} = 22$ km s^{-1} and (ii) for natal kick of 80 km s^{-1} and mass loss of ∼3 $M_\odot$ we get $e = 0.12$ and $V_{\rm spaceMWC656} = 36$ km s^{-1}. The above examples were obtained with our standard model, which assumes non-zero BH (but smaller than NS) kicks. Our model for non-zero kicks is based on the asymmetric mass ejection from pre-SN star. The amount of mass loss (that sets the natal kick value) is based on the SN models presented in Fryer et al. (2012). Apparently these models can explain both the eccentricity and space velocity of MWC 656. Obviously, our models with no BH natal kicks are also fully consistent with the eccentricity and peculiar space velocity estimates. Therefore, we cannot distinguish between the two models (asymmetric mass ejection versus no natal BH kicks).

3.4 On the origin of the Be phenomenon in Be-BH systems

The emission lines of regular MS Be stars are generally considered to result from an outflowing disc of a star rotating at or at a substantial fraction of its Keplerian rotation rate or break-up velocity (Rivinius, Carciofi & Martayan 2013). This raises the question about the origin of the spin of the Be star. This may either be reflecting the birth spin of the star or it may be the consequence of interaction in the binary system.

The first case is plausible, since young massive stars are observed to rotate at a wide range of rotation rates (e.g. Abt, Levato & Grosso 2002; Ramírez-Agudelo et al. 2013; Simón-Díaz & Herrero 2014). It does however require the Be star to retain its spin through all phases of binary interaction including the CE. This phase is poorly understood. Detailed stellar structure models show that rotating MS stars naturally tend to spin up their outer layers towards the Keplerian rotation rate. This does however require that the outer layers are well coupled with the contracting core. It also requires that angular momentum loss in the form of stellar winds is not significant, which is the case for most B-type MS stars and at low metallicity for the later O-type stars as well (Ekström et al. 2008; de Mink et al. 2013). In the currently favoured picture, this can cause stars that are rotating sufficiently fast to reach breakup as they evolve and show the emission phenomenon until they leave the MS.

The second case requires a phase of mass transfer from the progenitor of the current BH to the B star. Pols et al. (1991) showed that spin up by mass transfer is very efficient: accreting just a few per cent of its mass from an accretion disc is sufficient to bring a star to breakup. Simulations by Pols et al. (1991) and de Mink et al. (2013) show that, given the high binary frequency among massive stars, this is expected to be a very important or possibly even dominant channel for the formation of rapidly rotating stars (see also Shao & Li 2014).

In our models we find that none of our MWC 656-like systems (containing both B and Be stars) formed through a formation channel that included a phase of stable RLOF. So our simulations give preference to the first case, where the spin of the B star is the spin resulting from birth. However, it must be noted that in our model we rely on simplified prescriptions of the stellar structure and therefore an approximated treatment of the response of a star to RLOF. One possibility is spin-up during a (presumably short phase of) stable mass transfer preceding the CE. Another interesting alternative is stable mass transfer through atmospheric or wind RLOF (e.g. Abate et al. 2013).

3.5 The future evolution of MWC 656-like system

The fate of MWC 656-like system strongly depends on the secondary mass on ZAMS. We selected two broad evolutionary categories; binaries with relatively low-mass $10 < M_{2_{\rm zams}} < 13\,M_\odot$ and high-mass $13 < M_{2_{\rm zams}} < 16\,M_\odot$ secondaries. The summary of future evolution of MWC 656-like systems and the estimates of BH–NS formation chances are given in Table 2.

Table 2. Future evolution of MWC 656-like binaries.[a]

Channel	$f_{\rm form}$	Evolutionary history[b]	Mergers[c] CE/RLOF	Fate[d] (BH–NS): Close	Wide	Disrupted
B-BH:1a	15.4 per cent	CE1(4-1) SN1 MT2(14-2) MT2(14-9) ECSN2	0 per cent	0 per cent	15.4 per cent	0 per cent
B-BH:1b	23.1 per cent	CE1(4-1) SN1 MT2(14-2) SN2	0 per cent	0 per cent	0.5 per cent	22.6 per cent
B-BH:2a	7.7 per cent	CE1(4-1) SN1 CE2(14-4) MT2(14-7) SN2	0 per cent	5.6 per cent	0.7 per cent	1.4 per cent
B-BH:2b	53.8 per cent	CE1(4-1) SN1 CE2(14-2) MT2(14-7) SN2	38.4 per cent	10.7 per cent	1.3 per cent	3.4 per cent

[a]We list only formation channels of MWC 656-like systems which are defined by equation (4).
[b]Sequences of different evolutionary stages: CE1 and CE2: common envelope with a primary and secondary as a donor, respectively; MT2: non-conservative mass transfer with a secondary as a donor; SN1 and SN2: Type Ib/c supernova of the primary (BH formation) and secondary (NS formation), respectively; ECSN2: electron capture SN of secondary (NS formation). Numbers in parenthesis denote evolutionary stage of primary–secondary: 1 – main sequence, 2 – Hertzsprung gap, 4 – core helium burning, 7 – helium main sequence, 9 – helium giant branch, 13 – neutron star, 14 – black hole.
[c]This is probability that two binary components merge in RLOF or CE events that are encountered between the two SNe events.
[d]Outcome of future evolution of MWC 656-like systems; close (delay time from ZAMS to BH and NS merger shorter than 10 Gyr) or wide BH–NS systems or disrupted BH and NS objects may form.

3.5.1 Progenitors of wide BH–NS binaries

Here we describe, the future evolution of MWC 656-like systems with the initial (ZAMS) secondary mass smaller than 13 $M_\odot$. This group consists of ∼38 per cent of all MWC 656-like systems formed in Galactic disc, with 15.9 per cent forming wide BH–NS systems and 22.6 per cent are being disrupted in second SN.

We start with the binary consisting of a BH with mass $M_1 = 5.7\,M_\odot$, and a secondary star that has just entered HG with mass $M_2 = 10.2\,M_\odot$ (so right after MWC 656-like phase) and with separation $a = 153\,R_\odot$ ($P_{\rm orb} = 52.2$ d) and eccentricity $e = 0.28$.

The secondary quickly expands while crossing HG and it initiates stable RLOF on to the BH. Rapid expansion does not allow for tidal circularization. We circularize the system instantaneously at the onset of RLOF, we take the periastron distance as the new separation ($a = 110\,R_\odot$, $P_{\rm orb} = 34$ d) of circular orbit ($e = 0$). The accretion on to BH is Eddington limited, and the rest of mass leaves the system with the BH specific angular momentum. During RLOF the separation first decreases to $a = 101\,R_\odot$ ($P_{\rm orb} = 32$ d) and then increases to $a = 364\,R_\odot$ ($P_{\rm orb} = 263$ d). The binary components go through a mass ratio reversal, with BH mass $M_1 = 7.1\,M_\odot$ and the secondary mass $M_2 = 2.3\,M_\odot$ at the end of RLOF. The secondary becomes a naked helium star with CHeB that lasts about 4 Myr. The low-mass helium secondary begins to significantly expand after it becomes an evolved helium star (helium shell burning) and it initiates another episode of RLOF. At this point, the secondary mass decreases to $M_2 = 2.1\,M_\odot$ and the binary separations increases to $a = 423\,R_\odot$ ($P_{\rm orb} = 333$ d). As a result of the RLOF, the BH mass reaches $M_1 = 7.2\,M_\odot$ and secondary mass is depleted to $M_2 = 1.6\,M_\odot$, while the orbit expands to $a = 623\,R_\odot$ ($P_{\rm orb} = 608$ d). The secondary ends its evolution as an NS of a mass $M_2 = 1.26\,M_\odot$ created in ECSN. All binary systems survive the explosion as we assume no natal kick for ECSN and very little mass was lost in the process. This evolutionary channel is marked as 'B-BH:1a' in Table 2. We note the formation of wide BH–NS system with chirp mass of $M_{\rm c} = 2.4\,M_\odot$ and a very long merger time $t_{\rm merger} = 3.9 \times 10^8$ Gyr.

For slightly more massive secondaries ($M_{2_{\rm zams}} \approx 12\,M_\odot$) than in the above case, the second RLOF episode is avoided and an NS with mass $M_2 = 1.1\,M_\odot$ is created in a Type Ib/c SN explosion. The chance of survival of such a binary is only ∼2 per cent due to frequent natal kick disruptions. The systems that survive SN explosion form wide BH–NS binaries with merger times exceeding the Hubble time. This evolutionary channel is marked as 'B-BH:1b' in Table 2.

3.5.2 Progenitors of close BH–NS binaries

In this section, we describe the fate of MWC 656-like system with a secondary mass on ZAMS larger than 13 $M_\odot$. Such systems make up ∼62 per cent of the population of MWC 656-like binaries formed in Galactic disc. Although a significant fraction of these systems merge in ensuing CE (38.4 per cent), and some fraction gets either disrupted in the second SN explosion (4.8 per cent) or form wide BH–NS systems (2.0 per cent), a sizeable fraction forms close BH–NS systems (16.3 per cent).

We start with the binary consisting of a BH with mass $M_1 = 5.7\,M_\odot$, and a secondary star that just has entered HG with mass $M_2 = 13.5\,M_\odot$ (right after MWC 656-like phase) and with separation $a = 168\,R_\odot$ ($P_{\rm orb} = 58$ d) and eccentricity $e = 0.01$.

Typically, lower mass secondaries ($M_{2_{\rm zams}} \leq 14.5\,M_\odot$) evolve through HG and enter CHeB and then initiate CE (formation channel 'B-BH:2a'; see Table 2). The chances of survival of this CE are close to unity due to small CE envelope mass. Higher mass secondaries ($M_{2_{\rm zams}} \geq 14.5\,M_\odot$) initiate CE while still on HG ('B-BH:2b'). The chances of survival of this CE phase are only about one-third due to large CE mass. It is possible that instead of CE some of these systems evolve through fast (on thermal time-scale) but stable RLOF. In such a case these channels will contribute very little (if any) to the formation of close BH–NS binaries.

After CE, the secondary loses most of its mass and becomes a naked helium star with mass $M_2 = 3.3\,M_\odot$. The orbit is circularized and decreases in size to $a = 1.5\,R_\odot$ ($P_{\rm orb} = 1.7$ h). A very compact binary is formed. The CHeB secondary expands and initiates a stable RLOF. After ∼2 Myr the secondary becomes an evolved helium star. The RLOF continues. The BH mass increases to $M_1 = 6\,M_\odot$, while the secondary mass decreases to $M_2 = 1.6\,M_\odot$ and at the time of the SN explosion the orbit has expanded to $a = 4\,R_\odot$ ($P_{\rm orb} = 8.5$ h). After 16.5 Myr from the beginning of the evolution at ZAMS, the secondary explodes in Type Ib/c SN, forming an NS of a mass $M_2 = 1.1\,M_\odot$. Chances for a binary survival are very high as these systems are very compact.

For one particular natal kick, the post-SN orbit becomes eccentric $e = 0.46$ and the semimajor axis increases to $a = 5.7\,R_\odot$ ($P_{\rm orb} = 14.4$ h). The close BH–NS binary is formed with the chirp mass $M_{\rm c} = 2.1\,M_\odot$ and merger time $t_{\rm merger} = 1.5$ Gyr.

3.6 Future evolution of MWC 656

Based on the results presented in the above sections, we can describe the future evolution of a binary that resembles MWC 656

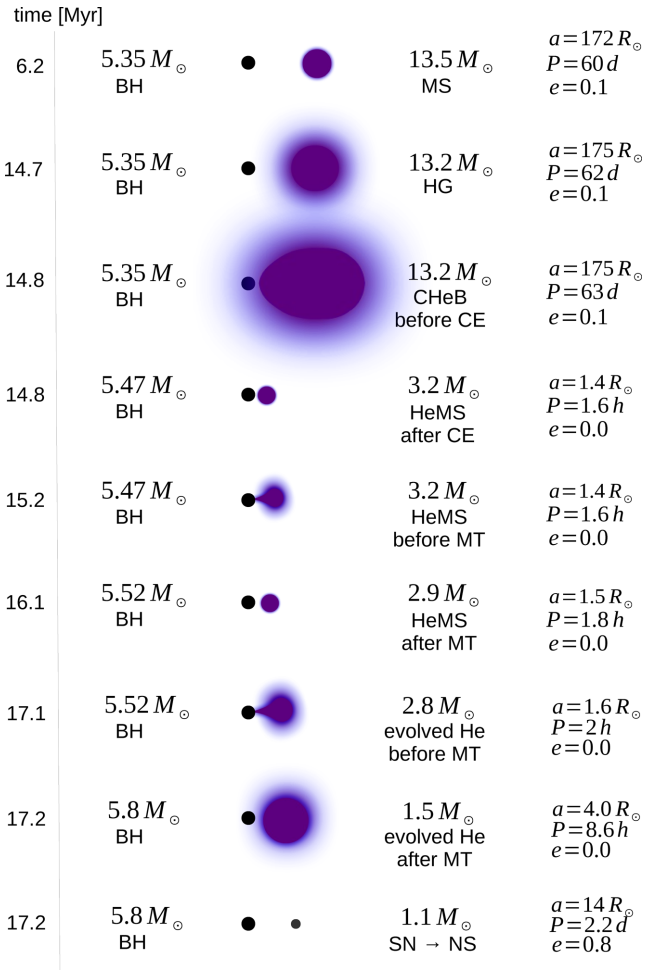

Figure 9. The future evolution of MWC 656 system (see Section 3.6). The binary evolves through CE and stable RLOF phase. If the binary survives CE phase the secondary star will form a light NS in SN explosion (1.1 $M_\odot$). Since CE significantly decreases the orbital separation, the binary is very likely to survive SN mass loss and natal kick and to form a close BH–NS system (probability of 77 per cent). We use the same notation as in Fig. 8, with the addition of MT – mass transfer, NS – neutron star.

(see Fig. 9). We start the evolution of the binary with a BH mass $M_1 = 5.35\,M_\odot$, B star mass $M_2 = 13.5\,M_\odot$, semimajor axis $a = 172\,R_\odot$ and eccentricity $e = 0.1$ and this results in an orbital period of $P_{\rm orb} = 60.37$ d (Casares et al. 2014). The parameters are all within the observational errors of the original observational estimates and allow for the system to evolve along our evolutionary channel 'B-BH:2a'. The massive primary ($M_{\rm zams} = 30$–$35\,M_\odot$) took ∼6.2 Myr to form a BH. A secondary MS lifetime is ∼14.8 Myr. This gives us a typical lifetime of the B-BH binary phase of $t_{\rm MWC656} = 8.6$ Myr. After finishing MS evolution, the secondary enters HG and starts to burn helium in its core. During this stage a CE phase is initiated. The orbit significantly decreases after CE and the secondary becomes a low-mass naked helium star. The secondary expands again while CHeB and initiates stable RLOF. A BH increases its mass during CE (by ∼0.12 $M_\odot$) and during stable RLOF (by ∼0.3 $M_\odot$) to $M_1 = 5.8\,M_\odot$. Finally, after $t_{\rm evol} = 17.2$ Myr from ZAMS the secondary explodes in Type Ib/c SN and forms an NS with mass $M_2 = 1.1\,M_\odot$. SN neutrino and mass loss (∼0.32 $M_\odot$) and natal kick (drawn from Maxwellian with $\sigma = 265$ km s^{-1}) may lead to a disruption of a binary (probability

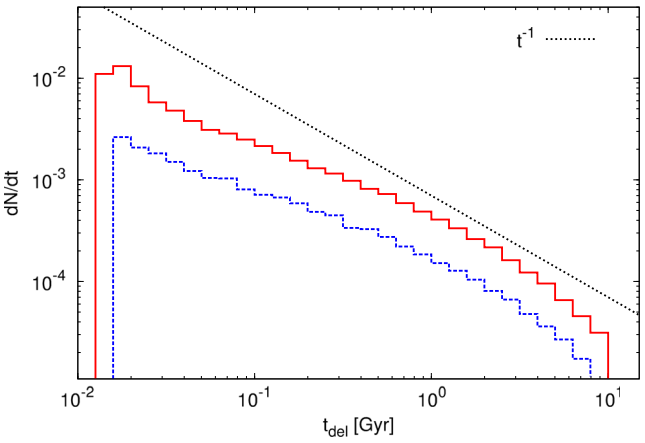

Figure 10. The delay time distribution for BH–NS systems formed out of MWC 656-like population defined by equation (4) (red solid curve; average 1.8 Gyr and median 0.8 Gyr) and for BH–NS systems formed from the system with exact observed MWC 656 properties as defined in Section 3.6 (blue dashed curve; average 2.0 Gyr and median 1.1 Gyr).

of 13.2 per cent), formation of wide non-coalescing BH–NS system (10.1 per cent) and formation of close: coalescing within 10 Gyr BH–NS system (76.7 per cent). There is very high probability of close BH–NS formation $f_{\rm close} = 0.77$ as the circular pre-SN orbit is very compact and hard to disrupt ($a = 4.0\,R_\odot$; $P_{\rm orb} = 8.6$ h). We use a high number of *Monte Carlo* experiments to assess these probabilities and we show the resulting distribution of delay times in Fig. 10. The close BH–NS systems that may form out of MWC 656 have average (and median) delay time of 1.9 Gyr (and 0.9 Gyr).

Note that initial stages of our prediction for future evolution of MWC 656 (Fig. 9) resemble a recently discovered ULX source: P13 in NGC 7793 (Motch et al. 2014). P13 is a binary with a 3–15 $M_\odot$ BH and ∼18–23 $M_\odot$ B9Ia companion. It was estimated that the system is experiencing the supercritical RLOF. The companion is proposed to be at the end of MS or at the beginning of HG. The orbital period is about 64 d. The only significant difference between P13 and MWC 656 is the mass of BH companion star. Since MWC 656 star has mass smaller than that in PG13, the RLOF will start later in its evolution. It is predicted that the onset of RLOF will begin when the star in MWC 656 will already finish crossing HG and will start CHeB. CE may be preceded by the short and stable high mass transfer rate phase (then the MWC 656 would resemble P13). However, it seems that due to the existence of deep convective envelope that forms during CHeB and quite high mass ratio (2.5) the development of CE is very likely.

Another object, SS433, was proposed to be a massive star engulfing a BH in its envelope (Clark, Barnes & Charles 2007). It may be the only known case of a massive binary undergoing CE. So far all the other binary mergers/CE events are restricted to low-mass stars (e.g. Kochanek, Adams & Belczynski 2014).

3.7 Empirical LIGO/Virgo detection rates

The lifetime of MWC 656 may be estimated from our evolutionary calculations presented in Section 3.6; $t_{\rm MWC656} = 8.6$ Myr. If we assume that only one such system is present currently in the Galaxy we obtain the Galactic birth rate of $\mathcal{R}_{\rm birth} \approx 1/t_{\rm MWC656}$ under assumptions that star formation in Galaxy was constant and nothing special or extraordinary was required to form MWC 656. We have shown in Section 3.6 that the probability of forming a close BH–NS

binary out of MWC 656 is $f_{\rm close} = 0.77$. Since the delay times are relatively short (median of the distribution is 0.9 Gyr; see Fig. 10) as compared with the Galactic disc age (10 Gyr), we can estimate the Galactic merger rate as

$$\mathcal{R}_{\rm MW} = f_{\rm close}\mathcal{R}_{\rm birth} = \frac{f_{\rm close}}{t_{\rm MWC656}} = 0.089\ {\rm Myr}^{-1}. \quad (5)$$

We have converted the Galactic merger rates to the advanced LIGO/Virgo detection rates ($\mathcal{R}_{\rm LIGO}$) assuming the constant density of Milky Way-like galaxies at the level $\rho_{\rm gal} = 0.01\ {\rm Mpc}^{-3}$ in local Universe. We have adopted $d_0 = 450$ Mpc as the advanced LIGO/Virgo horizon for NS–NS binary (optimally oriented source with signal-to-noise ratio of 8) with chirp mass $\mathcal{M}_{\rm c,nsns} \equiv (M_1M_2)^{3/5}(M_1+M_2)^{-1/5} = 1.2\,{\rm M}_\odot$ where individual NS masses are $M_1 = M_2 = 1.4\,{\rm M}_\odot$. The horizon for a double compact object with a given chirp mass $\mathcal{M}_{\rm c,dco}$ is calculated with $d = d_0(\mathcal{M}_{\rm c,dco}/\mathcal{M}_{\rm c,nsns})^{5/6}$. Finally, the detection rate is obtained with

$$\mathcal{R}_{\rm LIGO} = \rho_{\rm gal}\frac{4\pi}{3}\left(\frac{d_0}{f_{\rm pos}}\right)^3\left(\frac{\mathcal{M}_{\rm c,dco}}{\mathcal{M}_{\rm c,nsns}}\right)^{15/6}\mathcal{R}_{\rm MW}, \quad (6)$$

where factor $f_{\rm pos} = 2.26$ takes into account the non-uniform pattern of detector sensitivity and random sky orientation of sources. For our case of BH with $M_1 = 5.8\,{\rm M}_\odot$ and NS with mass $M_2 = 1.1\,{\rm M}_\odot$, we have $\mathcal{M}_{\rm c,dco} = 2.1\,{\rm M}_\odot$ and the corresponding detection rate of $\mathcal{R}_{\rm LIGO} = 0.115\ {\rm yr}^{-1}$. In other words, the existence of MWC 656 binary implies 1 BH–NS advanced LIGO/Virgo detection in 9 years.

This estimate is subject to a number of uncertainties. For example, if we lower mass of the B star $\sim$10 $\rm M_\odot$ then such a system will form only wide BH–NS binaries (see evolutionary channel 'B-BH:1a' in Table 2) and we get $\mathcal{R}_{\rm LIGO} = 0\ {\rm yr}^{-1}$. If we lower B star mass to $\sim$11–12 $\rm M_\odot$, such system will most likely get disrupted by core-collapse SN (see evolutionary channel 'B-BH:1b' in Table 2) and we also obtain $\mathcal{R}_{\rm LIGO} = 0\ {\rm yr}^{-1}$. These null rates are the direct result of our criterion on development of CE. For lower mass stars, instead of CE we encounter stable RLOF and therefore we form much wider systems that are either disrupted or do not merge within Hubble time. It is worth noting that the CE development and its inner mechanism is still far from being understood (Ivanova et al. 2013). On the other hand, we may increase the rate by increasing the B star mass to $\sim$15 $\rm M_\odot$ (this shortens the B lifetime to $t_{\rm MWC656} = 6.4$ Myr) and lowers the kick velocities by factor of 2 (this increases chance of SN survival to $f_{\rm close} = 0.92$) to obtain $\mathcal{R}_{\rm LIGO} = 0.187\ {\rm yr}^{-1}$ (1 detection in 5 years). Lower NS kicks in interacting binary systems are supported for example by the observed ratio of single to binary millisecond pulsars (Belczynski et al. 2010a).

4 DISCUSSION

We have studied the formation and future evolution of the first Be-BH binary system MWC 656. The study was carried out with population synthesis methods and it employed the standard model of single star and binary evolution.

The formation of the system requires just two distinctive evolutionary steps. First, the massive primary (a BH progenitor) initiates a CE that is needed for the formation of close binary with an orbital period similar to the one observed for MWC 656. Then, a Wolf–Rayet star (an exposed core of the primary) explodes in Type Ib/c SN and forms an $\sim$5 $\rm M_\odot$ BH and makes the system eccentric, again as observed for MWC 656. At this point, we note the formation of a massive binary consisting of a BH and a 10–16 $\rm M_\odot$ B/Be star.

Two competing scenarios are generally considered to explain the emission line phenomenon of Be stars. In both scenarios it is considered to be a direct result of rapid rotation and the presence of an outflowing disc. In the first scenario the B star is born as a substantially rapid rotator and retains this spin throughout its MS evolution. In the case of our evolutionary calculations, it would also have to retain its spin throughout the CE phase initiated by its companion. In the second scenario the B star was spin-up through interaction with the progenitor of the BH, most likely through accreting a small amount of mass. Just a few per cent of mass gain would be sufficient.

In our model we do not observe significant accretion and spin-up of the secondary star during the CE phase, giving some support to the first scenario to explain the Be phenomenon in this system. However, our rapid binary code relies on simplified prescriptions for stellar evolution and approximate treatment of the stars in response to mass transfer. It would be worth further investigating these formation channels in more detail with a full binary evolutionary code which properly solves the structure equations for both stars. Particularly interesting promising possibilities for the formation of Be-BH systems include a phase of stable mass transfer (and thus spin-up by mass transfer) preceding the CE phases (delayed CE) or a phase of wind or atmospheric RLOF.

At present the precise conditions for the Be phenomenon are not well understood. With our models we cannot make definite conclusions about the fraction of B stars that will show the phenomenon (and thus the fraction of B-BH binaries that appear as Be-BH binaries). In principle, explicit modelling of the stellar spins, the spin-up process and the moments of inertia will provide more information, for example as done by de Mink et al. (2013) and Shao & Li (2014) under the assumption of rigid body rotation. However, such simulations will not constrain the many remaining uncertainties. Among the most important unknowns is the mass transfer and the resulting spin-up during accretion. It is still not well understood how the accretion stream interacts with the star or the accretion disc and how the accreting star responds when its outer layers are spun up. Another important ingredient is the transfer of angular momentum throughout the star. Detailed stellar evolutionary models with and without interior angular momentum transport by magnetic fields give different results (e.g. Brott et al. 2011; Ekström et al. 2012). The situation is even less clear in the case of CE evolution. Particularly, it is unclear whether a star can accrete mass and spin up before or during the CE phase. (MacLeod & Ramirez-Ruiz 2015) find that the inspiralling object may increase its mass by a few per cent. This may be sufficient to spin up the accreting star (Packet 1981). As a general caveat the CE hydrodynamical simulations are still at the early stage and do not reproduce the observations (Passy et al. 2012). Finally, the initial distribution of stellar rotation rates is not well constrained. The observations for young massive stars show a bimodal distribution with most stars rotating with slow or moderate rates with a tail of rapid rotators reaching break-up velocity (e.g. Dufton et al. 2011, 2013; Ramírez-Agudelo et al. 2013; Simón-Díaz & Herrero 2014, and references therein). Considering all these uncertainties we opted for not following the spin evolution explicitly in this study. We investigated the formation channels of B-BH systems. A certain fraction of these will (intermittently) show the Be phenomenon. This fraction is uncertain. It may be as low as 0.3 if the ratio of Be stars to B stars is comparable to that observed in clusters. It may be higher if the interaction with the progenitor of the BH caused the Be phenomenon. A detailed investigation of the precise conditions for the occurrence of the Be phenomenon could prove to be very valuable.

Although it was found that several tens of B-BH binaries are currently residing in the Galactic disc, we find that there is only small probability (∼1/100) of having system resembling MWC 656 in terms of component masses and orbital period. In particular, in our simulations we find more systems with shorter orbital periods (∼5–10 d), less massive B stars (∼3–5 $M_\odot$) and slightly more massive BHs (∼7–8 $M_\odot$). For comparison, MWC 656 has orbital period of ∼60 d, Be star mass of 10–16 $M_\odot$ and BH mass of ∼5 $M_\odot$. If MWC 656 is representative of the intrinsic Galactic population of Be-BH binaries, it means that either our employed evolutionary model of massive stars or our adopted approach to CE and/or BH formation needs to be revised. We have employed non-rotating stellar models from Hurley et al. (2000) with stellar winds corrected for clumping from Vink, de Koter & Lamers (2001). If a massive primary happens to be a fast rotator, then our non-rotating models may not be a good choice, as one would expect smaller radii and larger cores for rapidly spinning stars. This would affect the development and the outcome of the CE phase and would also most likely lead to the formation of more massive BH (de Mink et al. 2013; Leitherer et al. 2014). The decreased stellar wind mass loss rates that we use are typically adopted in most recent evolutionary studies of massive stars. However, it appears that there may be some observational evidence for higher wind mass loss rates from massive stars (Eldridge, Izzard & Tout 2008). Had we adopted stronger winds, the primary core mass would decrease and to some extent it would counter-balance the evolutionary effects of fast rotation with the formation of a more massive BH. For CE evolution we have adopted the energy balance model of Webbink (1984) updated with the physical estimates of primary binding energy (Xu & Li 2010a,b). It appears that earlier claims that the core definition may change the post-CE binary separation by almost ∼2 orders of magnitude (Dewi & Tauris 2001) for stars with $M < 20\,M_\odot$ (NS progenitors) does not apply to more massive stars (i.e. BH progenitors; Wong et al. 2014). However, it is not at all clear that the energy balance model is good approximation for CE evolution, but no better model exists at the moment (Ivanova et al. 2013). For the BH formation we employ the rapid SN model from Fryer et al. (2012). This model explains observed mass gap between NSs and BHs (Belczynski et al. 2012a), the lack of compact objects in 2–5 $M_\odot$ mass range. Our model also allows us to reproduce the Galactic and extragalactic BH mass spectrum (Belczynski et al. 2010b). It is possible that the mass gap is caused by some observational bias involved in BH mass measurements as proposed by Kreidberg et al. (2012). However, we have shown that our results do not depend sensitively on this aspect of evolution (i.e. BH formation mass; see model V_4). We have adopted an asymmetric mass ejection mechanism for BH natal kicks and this results in small BH kicks (decreased with the amount of fall back). The empirically derived kick velocities for 14 Galactic BH binaries are inconclusive and the observational data allows for both small and high BH natal kicks (Belczynski et al. 2012b). Had we adopted high BH natal kicks (similar to those measured for single pulsars; e.g. Hobbs et al. 2005), the formation rates of B-BH binaries would decrease by large factor (∼1–2 orders of magnitude). In such the case we would expect very few Be-BH binaries to reside currently in the Galaxy. We have also tested the alternative model with BH natal kicks all set to zero. For this model we note a significant (a factor of ∼10; model V_3) increase of MWC 656-like systems currently predicted to reside in Galaxy.

With the recent discovery of a Oe star with a compact companion (Clark et al. 2015), we can await more Be-BH binaries to be found. When more Be-BH binaries are identified it will be essential to measure the intrinsic distribution of their orbital periods. Matching the intrinsic distribution with evolutionary models may allow us to improve our understanding of BH natal kicks and may offer some insights into the inner workings of CE, as these processes seem to be the most important factors affecting the formation of MWC 656-like systems and B-BH binaries in general.

The future evolution of MWC 656 offers a very interesting potential of forming a BH–NS system. In particular, close BH–NS systems are a class of gravitational-radiation sources for Advanced LIGO (Harry & the LIGO Scientific Collaboration 2010) and Virgo (Virgo Collaboration 2009) detectors, that are expected to start operation in a few years. We have estimated the formation rate of close (delay time from formation on ZAMS to BH–NS coalescence shorter than 10 Gyr) BH–NS systems from binaries similar to that of MWC 656. We have translated the formation rate to detection rate of BH–NS mergers by advanced LIGO/Virgo. The advanced LIGO/Virgo detection rate is found to be up to 1 detection in 5 years.

This empirically inferred detection rate is comparable to the rate obtained from analysis of Cyg X-3 binary (1 detection in 10 years; Belczynski et al. 2013) and is much higher than obtained for Cyg X-1 (1 detection in 100 years; Belczynski, Bulik & Bailyn 2011). These empirical estimates are based on existence of some particular binary stars and therefore they are only lower limits (i.e. formation of BH–NS only along one very specific formation channel) to the detection rate. However, it is encouraging that the observational evidence, although indirect, increases to support the existence of close BH–NS systems. It is now the total of three systems: Cyg X-1, Cyg X-3 and MWC 656 that were shown to be potential BH–NS progenitors. Other known high-mass XRBs were analysed and excluded as potential BH–NS progenitors (Belczynski, Bulik & Fryer 2012c). Recent population synthesis analysis of overall formation channels of double compact objects further supports the empirical evidence with estimates of BH–NS merger advanced LIGO/Virgo detection rates at the level 0.03–5.7 yr^{-1} (from 1 in 30 years to 6 per year; Dominik et al. 2015). Broader detection range is reported by Mennekens & Vanbeveren (2014): 0.04–484 yr^{-1} (from 1 in 25 years to 484 per year). So far there are no known stellar-origin BH–NS binaries. At the moment the only known potential BH–NS binary consists of a central Galactic supermassive BH (*Sagittarius A**) and its nearby magnetar PSR J1745−2900 (Eatough et al. 2013).

5 CONCLUSION

At present we know around 180 X–ray binaries (Ziolkowski 2014). For ∼120 of them the nature of compact object was confirmed to be an NS. Just in 2014 the first Be X–ray binary with a BH was discovered (MWC 656; Casares et al. 2014).

In this study, we have investigated the possible evolutionary scenarios leading to the formation of B-BH systems, part of which are Be-BH binaries. It was found that the B-BH progenitors experience CE phase. For the majority (90 per cent) of cases the CE donor is already an evolved star (CHeB), which increases chances of envelope ejection and a survival of the binary. In our simulations we used a code based on a non-rotating stellar models. Therefore, we are not able to resolve the issue of the origin of rapid rotation of Be stars. In our models it may be either connected to high initial star rotation or to spin up in CE (or pre-CE mass transfer) phase.

We checked the sensitivity of our results on the various evolutionary parameters assumed in our simulations. For all presented models, we expect up to few tens of B-BH systems to reside in the Galaxy at any given time, among which around 1/3 contain a Be star, but the chance to have a system very similar to the MWC 656 is

less than a few per cent. Future discoveries of Be-BH systems may allow us to determine the intrinsic distribution of orbital parameters and, by matching them with models, to improve our understanding of phases like CE and SN, which play an important role in the evolution of not only Be-BH binaries, but binaries in general.

We investigated the fate of systems similar to MWC 656. Future evolution of such systems may lead to the formation of BH–NS binaries. We find that 18 per cent (7 per cent) of such population will form close (wide) BH–NS systems, while the rest merges in the second CE phase or is disrupted in the second SN. We have repeated the prediction for a system exactly like MWC 656. Due to its favourable configuration, MWC 656 is very likely (∼77 per cent) to form a close BH-NS system that will merger within 10 Gyr.

These results make MWC 656 along with Cyg X-1 and Cyg X-3 the only reported potential progenitors of BH–NS binaries. The existence of MWC 656 alone implies that the detection of BH-NS mergers by advanced LIGO/Virgo can be as high as 1 in every 5 years.

ACKNOWLEDGEMENTS

The authors acknowledge the Texas Advanced Computing Center (TACC) at The University of Texas at Austin for providing computational resources. MG and KB acknowledge support from Polish Science Foundation 'Master2013' Subsidy. MG acknowledges support by Polish NCN grant Preludium (2012/07/N/ST9/04184). The work of KB was supported by the NCN grant Sonata Bis 2 (DEC-2012/07/E/ST9/01360), the National Science Foundation under grant no. PHYS-1066293 and the hospitality of the Aspen Center for Physics. JC acknowledges support by DGI of the Spanish Ministerio de Educación, Cultura y Deporte under grants AYA2010-18080, AYA2013-42627 and SEV-2011-0187. SdM acknowledges support for early stages of this study by NASA through an Einstein Fellowship grant, PF3-140105 and a Marie Sklodowska-Curie Reintegration Fellowship (H2020-MSCA-IF-2014, project id 661502). The work of IN and AH is partially supported by the Spanish Ministerio de Economía y Competitividad (MINECO) under grant AYA2012-39364-C02-01/02, and the European Union. MR acknowledges support by the Spanish MINECO under grant FPA2013-48381-C6-6-P. IR acknowledges support from the Spanish Ministry of Economy and Competitiveness (MINECO) and the Fondo Europeo de Desarrollo Regional (FEDER) through grant ESP2013-48391-C4-1-R. JMP acknowledges support by the Spanish MINECO under grant AYA2013-47447-C3-1-P and financial support from ICREA Academia. MB acknowledges support from the National Science Foundation under award HRD-1242090 and the hospitality of the Aspen Center for Physics.

REFERENCES

Abate C., Pols O. R., Izzard R. G., Mohamed S. S., de Mink S. E., 2013, A&A, 552, A26
Abt H. A., 1983, ARA&A, 21, 343
Abt H. A., 1987, in Slettebak A., Snow T. P., eds, IAU Colloq. 92: Physics of Be Stars. Cambridge Univ. Press, Cambridge, p. 470
Abt H. A., Levato H., Grosso M., 2002, ApJ, 573, 359
Artymowicz P., Lubow S. H., 1994, ApJ, 421, 651
Bailyn C. D., Jain R. K., Coppi P., Orosz J. A., 1998, ApJ, 499, 367
Belczynski K., Ziolkowski J., 2009, ApJ, 707, 870
Belczynski K., Kalogera V., Bulik T., 2002, ApJ, 572, 407
Belczynski K., Taam R. E., Kalogera V., Rasio F. A., Bulik T., 2007, ApJ, 662, 504
Belczynski K., Kalogera V., Rasio F. A., Taam R. E., Zezas A., Bulik T., Maccarone T. J., Ivanova N., 2008, ApJS, 174, 223
Belczynski K., Lorimer D. R., Ridley J. P., Curran S. J., 2010a, MNRAS, 407, 1245
Belczynski K., Bulik T., Fryer C. L., Ruiter A., Valsecchi F., Vink J. S., Hurley J. R., 2010b, ApJ, 714, 1217
Belczynski K., Dominik M., Bulik T., O'Shaughnessy R., Fryer C., Holz D. E., 2010c, ApJ, 715, L138
Belczynski K., Bulik T., Bailyn C., 2011, ApJ, 742, L2
Belczynski K., Wiktorowicz G., Fryer C. L., Holz D. E., Kalogera V., 2012a, ApJ, 757, 91
Belczynski K., Dominik M., Repetto S., Holz D. E., Fryer C. L., 2012b, preprint (arXiv:1208.0358)
Belczynski K., Bulik T., Fryer C. L., 2012c, preprint (arXiv:1208.2422)
Belczynski K., Bulik T., Mandel I., Sathyaprakash B. S., Zdziarski A. A., Mikołajewska J., 2013, ApJ, 764, 96
Brott I. et al., 2011, A&A, 530, A115
Casares J., Negueruela I., Ribó M., Ribas I., Paredes J. M., Herrero A., Simón-Díaz S., 2014, Nature, 505, 378
Chauville J., Zorec J., Ballereau D., Morrell N., Cidale L., Garcia A., 2001, A&A, 378, 861
Cheng Z.-Q., Shao Y., Li X.-D., 2014, ApJ, 786, 128
Clark J. S., Barnes A. D., Charles P. A., 2007, MNRAS, 380, 263
Clark J. S. et al., 2015, preprint (arXiv:1503.00930)
de Mink S. E., Langer N., Izzard R. G., Sana H., de Koter A., 2013, ApJ, 764, 166
Dewi J. D. M., Tauris T. M., 2001, in Podsiadlowski P., Rappaport S., King A. R., D'Antona F., Burderi L., eds, ASP Conf. Ser. Vol. 229, Evolution of Binary and Multiple Star Systems. Astron. Soc. Pac., San Francisco, p. 255
Diehl R. et al., 2006, Nature, 439, 45
Dominik M., Belczynski K., Fryer C., Holz D. E., Berti E., Bulik T., Mandel I., O'Shaughnessy R., 2012, ApJ, 759, 52
Dominik M. et al., 2015, ApJ, 806, 263
Dufton P. L. et al., 2011, ApJ, 743, L22
Dufton P. L. et al., 2013, A&A, 550, A109
Duquennoy A., Mayor M., 1991, A&A, 248, 485
Eatough R. P. et al., 2013, Nature, 501, 391
Ekström S., Meynet G., Maeder A., Barblan F., 2008, A&A, 478, 467
Ekström S. et al., 2012, A&A, 537, A146
Eldridge J. J., Izzard R. G., Tout C. A., 2008, MNRAS, 384, 1109
Fabregat J., Torrejón J. M., 2000, A&A, 357, 451
Frémat Y., Neiner C., Hubert A.-M., Floquet M., Zorec J., Janot-Pacheco E., Renan de Medeiros J., 2006, A&A, 451, 1053
Fryer C. L., Belczynski K., Wiktorowicz G., Dominik M., Kalogera V., Holz D. E., 2012, ApJ, 749, 91
Granada A., Ekström S., Georgy C., Krtička J., Owocki S., Meynet G., Maeder A., 2013, A&A, 553, A25
Harry G. M., the LIGO Scientific Collaboration, 2010, Class. Quantum Gravity, 27, 084006
Hayasaki K., Okazaki A. T., 2006, MNRAS, 372, 1140
Hobbs G., Lorimer D. R., Lyne A. G., Kramer M., 2005, MNRAS, 360, 974
Hummel W., Hanuschik R. W., 1997, A&A, 320, 852
Hummel W., Vrancken M., 1995, A&A, 302, 751
Hurley J. R., Pols O. R., Tout C. A., 2000, MNRAS, 315, 543
Ivanova N., Chaichenets S., 2011, ApJ, 731, L36
Ivanova N. et al., 2013, A&AR, 21, 59
Kato S., 1983, PASJ, 35, 249
Keller S. C., Wood P. R., Bessell M. S., 1999, A&AS, 134, 489
Kennicutt R. C., Jr, 1998, ARA&A, 36, 189
Kobulnicky H. A., Fryer C. L., Kiminki D. C., 2006, preprint (arXiv:astro-ph/0605069)
Kochanek C. S., Adams S. M., Belczynski K., 2014, MNRAS, 443, 1319
Kreidberg L., Bailyn C. D., Farr W. M., Kalogera V., 2012, ApJ, 757, 36
Kroupa P., Weidner C., 2003, ApJ, 598, 1076
Leitherer C., Ekström S., Meynet G., Schaerer D., Agienko K. B., Levesque E. M., 2014, ApJS, 212, 14
MacLeod M., Ramirez-Ruiz E., 2015, ApJ, 803, 41

McMillan P. J., 2011, MNRAS, 414, 2446
McSwain M. V., Gies D. R., 2005, in Ignace R., Gayley K. G., eds, ASP Conf. Ser. Vol. 337, The Nature and Evolution of Disks Around Hot Stars. Astron. Soc. Pac., San Francisco, p. 270
Maeder A., Grebel E. K., Mermilliod J.-C., 1999, A&A, 346, 459
Marco A., Negueruela I., 2013, A&A, 552, A92
Martayan C., Frémat Y., Hubert A.-M., Floquet M., Zorec J., Neiner C., 2006, A&A, 452, 273
Mennekens N., Vanbeveren D., 2014, A&A, 564, A134
Meynet G., Maeder A., 2005, in Ignace R., Gayley K. G., eds, ASP Conf. Ser. Vol. 337, The Nature and Evolution of Disks Around Hot Stars. Astron. Soc. Pac., San Francisco, p. 15
Misiriotis A., Xilouris E. M., Papamastorakis J., Boumis P., Goudis C. D., 2006, A&A, 459, 113
Motch C., Pakull M. W., Soria R., Grisé F., Pietrzyński G., 2014, Nature, 514, 198
Negueruela I., 1998, A&A, 338, 505
Negueruela I., Okazaki A. T., 2000, in Smith M. A., Henrichs H. F., Fabregat J., eds, ASP Conf. Ser. Vol. 214, IAU Colloq. 175: The Be Phenomenon in Early-Type Stars. Astron. Soc. Pac., San Francisco, p. 713
Negueruela I., Okazaki A. T., 2001, A&A, 369, 108
Negueruela I., Okazaki A. T., Fabregat J., Coe M. J., Munari U., Tomov T., 2001, A&A, 369, 117
Nelemans G., Tauris T. M., van den Heuvel E. P. J., 1999, A&A, 352, L87
Okazaki A. T., 1996, PASJ, 48, 305
Okazaki A. T., 1997, A&A, 318, 548
Okazaki A. T., Negueruela I., 2001, in Giacconi R., Serio S., Stella L., eds, ASP Conf. Ser. Vol. 234, X-ray Astronomy 2000. Astron. Soc. Pac., San Francisco, p. 281
Özel F., Psaltis D., Narayan R., McClintock J. E., 2010, ApJ, 725, 1918
Packet W., 1981, A&A, 102, 17
Passy J.-C. et al., 2012, ApJ, 744, 52
Pols O. R., Cote J., Waters L. B. F. M., Heise J., 1991, A&A, 241, 419
Portegies Zwart S. F., 1995, A&A, 296, 691
Porter J. M., 1996, MNRAS, 280, L31
Porter J. M., 1999, A&A, 348, 512
Porter J. M., Rivinius T., 2003, PASP, 115, 1153
Ramírez-Agudelo O. H. et al., 2013, A&A, 560, A29
Rappaport S., van den Heuvel E. P. J., 1982, in Jaschek M., Groth H.-G., eds, Proc. IAU Symp. 98, Be Stars. Reidel, Dordrecht, p. 327
Reid M. J., Brunthaler A., 2004, ApJ, 616, 872
Reid M. J. et al., 2014, ApJ, 783, 130
Reig P., 2011, Ap&SS, 332, 1
Reig P., Fabregat J., Coe M. J., 1997, A&A, 322, 193
Rivinius T., Carciofi A. C., Martayan C., 2013, A&AR, 21, 69
Robitaille T. P., Whitney B. A., 2010, ApJ, 710, L11
Sana H. et al., 2012, Science, 337, 444
Shao Y., Li X.-D., 2014, ApJ, 796, 37
Simón-Díaz S., Herrero A., 2014, A&A, 562, A135
Stella L., White N. E., Rosner R., 1986, ApJ, 308, 669
Struve O., 1931, ApJ, 73, 94
Townsend R. H. D., Owocki S. P., Howarth I. D., 2004, MNRAS, 350, 189
van Leeuwen F., 2007, A&A, 474, 653
Vink J. S., de Koter A., Lamers H. J. G. L. M., 2001, A&A, 369, 574
Virgo Collaboration 2009, Virgo Technical Report VIR-0027A-09, Advanced Virgo Baseline Design
Waters L. B. F. M., Pols O. R., Hogeveen S. J., Cote J., van den Heuvel E. P. J., 1989, A&A, 220, L1
Webbink R. F., 1984, ApJ, 277, 355
Wisniewski J. P., Bjorkman K. S., 2006, ApJ, 652, 458
Wong T.-W., Valsecchi F., Ansari A., Fragos T., Glebbeek E., Kalogera V., McClintock J., 2014, ApJ, 790, 119
Xu X.-J., Li X.-D., 2010a, ApJ, 716, 114
Xu X.-J., Li X.-D., 2010b, ApJ, 722, 1985
Ziolkowski J., 2002, Mem. Soc. Astron. Ital., 73, 1038
Ziolkowski J., 2014, in Proc. 10th International Workshop on Multifrequency Behaviour of High Energy Cosmic Sources, Be/X-Ray Binaries with Black Holes in the Galaxy and in the Magellanic Clouds. Czech Technical University, Prague, p. 175
Ziółkowski J., Belczyński K., 2011, in Giovannelli F., Mannocchi G., eds, Proc. Vulcano Workshop 2010, Frontier Objects in Astrophysics and Particle Physics. Ital. Phys. Soc., Editrice Compositori, Bologna p. 511
Zorec J., Briot D., 1997, A&A, 318, 443

APPENDIX A: CONSTRAINTS ON THE SN EXPLOSION IN MWC 656

In this appendix, we report on the space velocity of MWC 656 and on constraints on the SN explosion that originated the BH in this system.

The position of MWC 656 in the ICRS (epoque J2000) according to van Leeuwen (2007) is

$$\alpha = (224\,257.302\,95 \pm 0.67)\ \mathrm{mas}$$
$$\delta = (+444\,318.2525 \pm 0.72)\ \mathrm{mas}, \quad \text{(A1)}$$

where α and δ means right ascension and declination, respectively. Its proper motion from the same reference is

$$\mu_\alpha \times \cos(\delta) = (-3.56 \pm 0.72)\ \mathrm{mas\ yr^{-1}}$$
$$\mu_\delta = (-4.05 \pm 0.76)\ \mathrm{mas\ yr^{-1}}. \quad \text{(A2)}$$

From Casares et al. (2014), the radial velocity of MWC 656 is $(-14.1 \pm 2.1)\ \mathrm{km\,s^{-1}}$ and its distance is (2.6 ± 0.6) kpc.

The Galactic rotation curve of Model A5 in table 4 of Reid et al. (2014) provides

$$\mathrm{R}_\odot = (8.34 \pm 0.16)\ \mathrm{kpc}$$
$$\Theta_\odot = (240 \pm 8)\ \mathrm{km\ s^{-1}}$$
$$d_{\Theta_\odot}/d_{\mathrm{R}_\odot} = (-0.2 \pm 0.4)\,\mathrm{km\,s^{-1}\,kpc^{-1}}. \quad \text{(A3)}$$

The same model provides a peculiar space velocity of the Sun relative to the local standard of rest of:

$$U_\odot = (10.7 \pm 1.8)\ \mathrm{km\ s^{-1}}$$
$$V_\odot = (15.6 \pm 6.8)\ \mathrm{km\ s^{-1}}$$
$$W_\odot = (8.9 \pm 0.9)\ \mathrm{km\ s^{-1}}. \quad \text{(A4)}$$

The coordinates adopted for the North Galactic Pole and Zero longitude are those listed in the appendix of Reid & Brunthaler (2004):

$$\alpha_{\mathrm{pole}} = 12^{\mathrm{h}}\,51^{\mathrm{m}}\,26\overset{\mathrm{s}}{.}282 = 192.859\,5083\ \mathrm{deg}$$
$$\delta_{\mathrm{pole}} = +27^\circ\,07'\,42\overset{''}{.}01 = 27.128\,336\,11\ \mathrm{deg}$$
$$\theta = 122.932\ \mathrm{deg}. \quad \text{(A5)}$$

Using all these values, we obtain a peculiar space velocity of MWC 656:

$$v_{\mathrm{space_{MWC656}}} = (22.5 \pm 14.9)\ \mathrm{km\ s^{-1}}. \quad \text{(A6)}$$

The uncertainty was calculated using values listed in Table A1, which added in quadrature give $14.9\ \mathrm{km\,s^{-1}}$. Therefore, the measurement of space velocity is only significant at the 1.5σ level. Even for a fixed distance with no uncertainty the total uncertainty is $12.7\ \mathrm{km\,s^{-1}}$, providing not even a 2σ detection. To obtain a 3σ detection it is required to provide null uncertainties for both the distance and the Galactic rotation curve.

Table A1. The contribution of individual uncertainty to the space velocity uncertainty of MWC 656.

Considered uncertainty	Measured value ($km\,s^{-1}$)
Proper motion	5.2
Radial velocity	1.7
Distance	7.8
Galactocentric distance	0.5
Galactic rotation of the Sun	6.8
Galactic rotation around MWC 656	7.0
Peculiar space velocity of Sun	5.8

The masses and orbital parameters of MWC 656 from Casares et al. (2014) are

$$M_1 = (13 \pm 3)\,M_\odot$$
$$M_2 = (5.3 \pm 1.5)\,M_\odot$$
$$P = (60.37 \pm 0.04)\mathrm{d}$$
$$e = 0.10 \pm 0.04. \quad \text{(A7)}$$

Considering the large orbital period and the small eccentricity, it is reasonable to assume that the current value of eccentricity is similar to the one just after the SN explosion, e_{postSN}. In such a case, the mass lost during the SN explosion is similar to or slightly above

$$\Delta_M = e_{\mathrm{postSN}}(M_1 \cdot M_2) = (1.8 \pm 0.8)\,M_\odot. \quad \text{(A8)}$$

Using the formalism described in Nelemans, Tauris & van den Heuvel (1999) (although the orbital period here is much larger than 7 d) we find reduced mass, re-circularized period and initial orbital period:

$$\mu = 0.91 \pm 0.03$$
$$P_{\mathrm{recirc}} = (59.5 \pm 0.7)\,\mathrm{d}$$
$$P_{\mathrm{init}} = (49 \pm 4)\,\mathrm{d}. \quad \text{(A9)}$$

Table A2. The contribution of individual uncertainty to the uncertainty of the mass lost in the SN explosion of MWC 656.

Considered uncertainty	Measured value ($M_\odot$)
Space velocity	2.6
Mass of Be star	2.0
Mass of BH	0.6
Re-circularized period	0.02

With all these parameters we obtain an expected MWC 656 space velocity of

$$v_{\mathrm{exp_{MWC656}}} = (10.2 \pm 4.7)\,km\,s^{-1} \quad \text{(A10)}$$

to be compared to the measured space velocity of (22.5 ± 14.9) $km\,s^{-1}$ from equation (A6).

Both values are compatible at the 1σ level, indicating that there is no need of any additional kick to produce the observed space velocity with a symmetric SN explosion with a mass loss of $(1.8 \pm 0.8)\,M_\odot$.

If we use the equation 7 from Nelemans et al. (1999) to compute the mass lost in the SN explosion considering the measured space velocity and all other values with their corresponding uncertainties, we obtain

$$\Delta_M = (4.0 \pm 3.4)\,M_\odot, \quad \text{(A11)}$$

where the uncertainty was calculated using values from Table A2. As expected, this is compatible with the value derived from the current masses and the eccentricity of the orbit.

In conclusion, everything seems compatible with no kick and a moderate mass loss of a few solar masses to produce both the observed eccentricity and the space velocity of MWC 656.

This paper has been typeset from a TEX/LATEX file prepared by the author.